

# **3<sup>rd</sup> European Academic Symposium on EAF Steelmaking**

29-30 May 2018, Aachen, Germany



**Abstract booklet**

## Recent developments on the graphite electrode market in the EU

T. Willms, T. Reichel, T. Echterhof, H. Pfeifer  
RWTH Aachen University  
willms@iob.rwth-aachen.de

### INTRODUCTION

In addition to the blast furnace converter route, electric steel production in the electric arc furnace is one of the two main production routes for crude steel. In 2016, the share of the world via the electric steel route was around the world 34 % of crude steel, equivalent to approx. 407 million tonnes of crude steel. [1] For the crude steel production in the electric arc furnace, electrical energy is used to melt mostly steel scrap. Graphite electrodes are used to transfer the required energy. Graphite is pure carbon. On the one hand, it can be made from carbonaceous raw materials; on the other hand, it is also present as a natural resource. Its good electrical conductivity and high temperature resistance characterize graphite. Therefore, graphite is used in many areas.

In addition as electrode in the electric arc furnace, graphite is used, for example as anode in lithium ion accumulators or in the fused-salt electrolysis of alumina. The demand for graphite increases on the one hand by the electrification of road traffic, on the other by the increasing production of alumina. Inter alia, these two factors lead to a shortage of graphite electrodes in steelmaking and increasing prices.

### Raw materials and production of graphite electrodes

For all types of graphite, naturally occurring natural graphite and anthracites are suitable as raw material, whereas cokes and carbon blacks are artificially produced starting materials. The main component of graphite electrodes are highly anisotropic needle cokes. These are ideally suited because of their needle-like structure, since it depends on the electrode on a very high electrical, mechanical and thermal capacity. The delayed coking process produces needle coke industrially. Here, residual residues of crude oil or coal tar pitch, a by-product of coke production, are delayed in refineries and gently coked.

However, all needle cokes still contain a considerable proportion of volatile constituents and hydrogen of about 5 to 12% by mass. This leads to mass losses in the event of subsequent heating and ultimately to pore and crack formation. [2]

Needle coke is not sinterable under normal conditions, which is why it must be connected to each other via binder bridges by means of binders. Suitable binders are usually coal tar pitch and phenolic resins.

The manufacturing process of graphite electrodes is divided into the processing of raw materials, the shaping process, baking and graphitizing as well as the final processing of the products.

In the first step, the needle coke is milled and sieved to the necessary grain size and then mixed with binders. Due to the anisotropy of the needle coke, the shaping process, in graphite electrode production, must ensure intentional alignment of the particles. The subsequent electrical conductivity of the electrode is the most important prerequisite for the functionality and is defined by the shape. For this reason, all graphite electrodes are extruded, whereby the needles are longitudinally aligned and arranged in a circle. Therefore, single- or twin-screw extruders are used. The thermal treatment is divided into two processes, the baking and the final graphitizing. During the baking the material is heated up 1300 °C in several steps. For the final graphitizing of the electrodes temperatures up to 3000 °C are necessary. In the last step of the electrode, production is machined to its final dimensions as well as the sockets for connection between the sections of each electrode. [2]

### Needle coke market

As mentioned in the previous section needle coke is the main raw material for the electrode production. The price for a ton of needle coke in 2017 is 2600 €. Compared to the previous year, when a price of 370 €/t was requested, a price increase of 600% can be seen [3]. Not only supply and demand play a greater-term role in this significant price increase. Rather, a combination of supply and demand, political decisions and natural disasters are determining factors in the world market of needle coke.

In Summation, these are the main factors for the increasing prices:

- Oligopolistic market structure [4]
- Energy intensive production, only profitable at production sites with low energy costs
- Rising demand because of the increasing production of aluminium and lithium-ion-batteries [5]
- Damage of production sites in Houston (31,9% of worldwide needle coke production) caused by hurricane Harvey in 08/17 [6]

- Closing of production sites in China due to new environmental regulations [7]
- Increasing steel-production on the EAF-route in China [1]

### Graphite electrode market

For the past decade, the graphite electrode manufacturers have been struggling with falling prices and fierce competition from China and Japan. There was a continuous oversupply of electrodes and the capacities of the manufacturers were never fully utilized.

At the beginning of 2017, the price of graphite electrodes rose from 1,700 €/t within months to over 29,200 €/t in September 2017 to € 37,570 €/t [4, 7, 8]. The main reason is the increasing needle coke price. Graphite electrodes mainly consist of petroleum coke-based needle cokes, whereby the cost of the starting material, depending on the source [4, 7, 8], is 40% to 70% of the total geothermal costs. But the increase of the needle coke price would only let to a price of 11,000 €/t [4]. Besides the factors which also let to an increased needle coke price are the following factors:

- Oligopolistic market structure [4]
- Reduction of worldwide production capacity, especially in China (30% in 2017) [9]
- Timely purchase of steel plants at the end of 2017 and panic buying in fear of more increasing prices
- Increasing steel production in the EU due to reduction of steel exports from China [4]
- Continuous decreasing exports of graphite electrodes from China [9]

### Conclusion and outlook

The raw material needle coke causes approximately 40% to 70% of the electrode costs and has risen rapidly in 2017 due to a natural disaster, increasing demand from other industries and political decisions in China. At the same time, in addition to years of hard price competition and continuous capacity reductions, these decisions are leading to a shortage of graphite electrode production. These factors, combined with an oligopolistic market situation and no alternatives as substitutes, exacerbate the market around the graphite electrode.

A constant price level is likely of needle coke such as graphite electrodes for the next two years. It has to be seen which new capacities will come onto the market after these two years and what effects an increased availability of needle coke will have on the price. The increased and sustained demand for needle coke and the increasing number of EAFs in China are unlikely to bring the price back down to its 2016 price of 1,700 €/t even after two years. Graphite electrode prices of an estimated 10,000 €/t to 20,000 €/t are

quite likely. Currently, in May 2018, a German electrode manufacturer reports that the situation has eased compared to 2017. Prices are not rising any further, although they are still consistently high. Also of interest is the development of the lithium-ion battery sector.

### REFERENCES

- [1] **World Steel Association:** Steel statistical yearbook 2017, Brussels (Belgium), 2017
- [2] **Kindler, A.; Hoffmann, W.; Vesper, W.; Walter, S.:** Feinkorngraphite Moderne Werkstoffe und ihre technische Anwendung, 2nd edition, Verlag Moderne Industrie, Landsberg, 2010
- [3] **Martinez Canorea, I.:** Breaking down the Graphite Surcharge Cost for Stainless Steel, URL: <https://agmetalmminer.com/2017/10/26/graphite-surcharge-cost-electrodes-outokumpu-ak-steel-sgl-sdk-graftech/>, retrieved on 22.05.2018
- [4] **Steelmint.:** Will Indian Graphite Electrode Price Graph be Flat or Curvy in 2018?, URL: <http://events.steelmintgroup.com/will-indian-graphite-electrode-price-graph-flat-curved-2018/>, retrieved on 22.05.2018
- [5] **Grand View Research:** Needle Coke Market Analysis, Market Size, Application Analysis, Regional Outlook, Competitive Strategies, and Forecasts, 2015 To 2022, URL: <https://www.grandviewresearch.com/industry-analysis/needle-coke-market>, retrieved on 22.05.2018
- [6] **Jill Disis, M. E. a. C. I.:** 10 refineries close as Harvey drenches Texas energy hub, URL: <http://money.cnn.com/2017/08/27/news/economy/tropical-storm-harvey-texas-oil-gas/index.html>, retrieved on 22.05.2018
- [7] **Shenoy, D.:** Story: How the Pollution in China Caused a 3x increase in Graphite Electrode Profits in a Year, URL: <https://capitalmind.in/2017/11/story-pollution-china-caused-3x-increase-graphite-electrode-profits-year/>, retrieved on 22.05.2018
- [8] **Afonso, S.:** These Stocks Have Surged 400% This Year — But the Best May Be Yet to Come, URL: <https://www.bloomberg.com/news/articles/2017-10-03/these-top-stocks-seen-extending-rally-after-400-surge-this-year>, retrieved on 22.05.2018
- [9] **Manolo Serapio Jr, T. D. r.:** The graphite fix: Inside China's newest commodity addiction, URL: <https://www.reuters.com/article/us-china-steel-graphiteelectrode/the-graphite-fix-inside-chinas-newest-commodity-addiction-idUSKCN1BW0S2>, retrieved on 22.05.2018

## Slag sampling and analysis from a lab-scale Electric Arc Furnace

Carrie Jonsson, Nils Andersson, Pär Göran Jönsson, Anders Tilliander

KTH Royal Institute of Technology, ITM-MSE-Unit of Processes, 100 44 Stockholm, Sweden  
carriej@kth.se

### INTRODUCTION

Electric arc furnaces (EAF) are used in steelmaking to melt down raw materials such as steel scrap in order to produce new steels. Synthetic slags are used to refine and clean the molten steel in the steelmaking process.

It is beneficial that the slag composition can be known as early as possible in the EAF process, so that actions and decisions can be taken promptly for an efficient process control of EAF. However, this is still a challenge today, because no steel companies have yet incorporated direct slag composition data in an online process control system for the EAF process. Therefore, this work is part of an attempt to obtain a better understanding of change of the slag components, based on measurements in a lab-scale EAF. The ultimate goal of the work is to make it possible to measure the slag composition online with optical emission spectrometry (OES) in a full-scale EAF.

By testing the variations of slag levels and slag compositions, we can learn how these parameters affect the plasma measurements with optical emission spectrometry. The comparison between how slag level and compositions can affect OES measurement is still in progress. (OES measurement will be presented by participant from the University of Oulu.)

A large amount of energy is required by the electric arc furnace in the melting process. Light and heat are generated by the electric arc. The arc and plasma consist of a highly radiant mixture of free electrons, ions, atoms and molecules. A plasma occurs if a gas is heated strongly [1]. The electric arc provides this energy for the melting process in an industrial EAF.

### MATERIALS AND METHODS

A lab-scale EAF at KTH with 10 kg capacity (Figure 1), was used for the trials. It was equipped with induction heating and an integrated water cooling system.

**Experimental Procedure.** A graphite crucible was lined with refractory material and allowed to dry and sinter before the melting of steel and slag formers. At the beginning of the trial, carbon steel (5 kg), carbon (200 g) were added into the graphite crucible. Thereafter, induction heating was employed in order

to achieve a sufficiently high temperature for the melting of carbon steel, carbon and slags. Slag formers of ca. 215 g per batch comprised of (in wt %) CaO 40, MgO 10, SiO<sub>2</sub> 35, Al<sub>2</sub>O<sub>3</sub> 15 were added into the graphite crucible. Variations of slag levels were tested. Specifically, 3-5 batches of slag formers were added stepwise to vary the slag level from 15 mm, 20 mm and 25 mm in the crucible. An addition, 50 g CaO per addition were added twice after a 25 mm slag level had been reached. Thereafter, a ladle slag (79 g and 84 g respectively) were added in the end in order to increase the variation of the slag composition. Oxygen lancing was introduced into the steel melt to create a foaming which is similar to what is found in an electric arc furnace.

A welding power source, ESAB LHH400 was used to supply a 200-300A direct current (DC) to the two graphite electrodes in the lab-scale EAF. Also, a controller was used to adjust the height of the two graphite electrodes from the melt. This functioned not only as a height adjustment of the electrodes, but also as a means to initiate the arc.

The temperature of the steel melt was measured repeatedly with a S-type thermocouple via a lance (Heraeus Electro-Nite), before each slag sampling. Also, three different methods were tested to sample slag. Specifically, the slag samples were obtained by using rebars, slag rakes and quartz tubes.

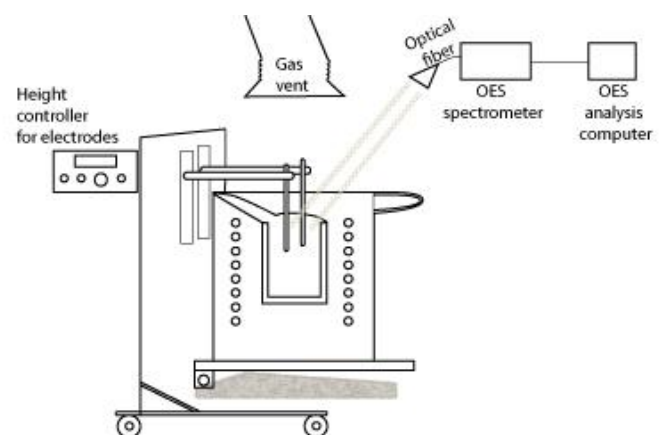


**Figure 1. Lab-scale Electric Arc Furnace at KTH.**

The composition of the slag samples were analysed with x-ray fluorescence (XRF). In total, 10 sets of slag samples were analysed with XRF. 10 grams from

each samples were first crushed into powder with a particle size <150µm and then 1 gram of each sample was analysed.

Characterization and semi-quantitative analyses of the slag samples were performed using a Hitachi TM3000 scanning electron microscope (SEM) equipped with an energy dispersive spectroscopy (EDS) analyser.

## RESULTS AND DISCUSSIONS

The added slag formers had a basicity ( $\text{CaO}+\text{MgO} / \text{SiO}_2+\text{Al}_2\text{O}_3$ ) of 1, where their weight percentage values are presented in Figure 2. Each batch of slag formers produced approximately a 5 mm slag level in the lined crucible. In 3-5 batches of slag formers the slag levels varied from 15 to 25 mm. A foaming of slag was tested with oxygen injection in trial number 10. The fraction of added ladle slag (containing  $\text{Cr}_2\text{O}_3$ ,  $\text{FeO}$ ,  $\text{MnO}$ ,  $\text{SO}_3$ ,  $\text{TiO}_2$ , F, BaO) in number 8 constituted 0,9 wt % of the slag. For trials number 9 and 10 the fraction of ladle slag was increased to 1.7 wt %.

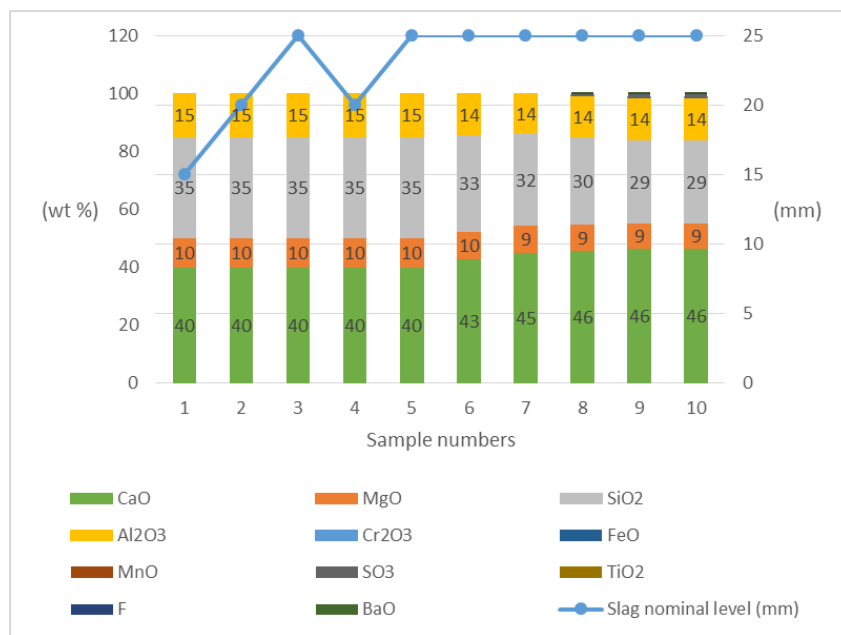


Figure 2. Slag formers added in wt % and nominal slag level.

**Temperature.** Temperatures measured right before each slag samplings are shown in Table 1. The temperature was an important parameter because it can affect the slag characteristic and foaming ability [2].

Table 1. Temperature (°C) of the steel melt.

Sample	1	2	3	4	5	6	7	8	9	10*
Temperature	1595	1558	1553	1585	1566	1534	1404	1564	1644	1490

Note: 10\* slag foaming

**Slag foaming.** Gas development in the slag phase created a condition for slag foaming. It was the purpose to create CO gas by adding carbon with the steel in the beginning of the experiment. Reaction between the dissolved carbon with the injected oxygen forms the reaction products CO (g) alternatively CO<sub>2</sub> (g) [2].

**Sampling methodology.** After tested, the different slag sampling methods had both advantages and disadvantages. With rebars and slag rakes, clean slag samples were obtained but the sample amounts were low. On the other hand, with quartz tubes a larger amount of slag sample could be obtained but the slag sample and the quartz tube wall adhered to each others. When separating the slag sample from the quartz tube material the slag sample was contaminated. Therefore, a new slag sampling method should be developed in order to obtain a large enough slag sample, such as by using a scoop or a ladle-like tool for slag sampling inside the crucible.

**Slag analysis.** The slag samples that were analysed with XRF and SEM showed a high content of MgO and it was higher than the MgO in the slag formers. This indicated that a dissolution of MgO from the lined refractory material occurred at the high temperatures. Therefore, the crucible should be lined with another type of material or a new crucible material should be used for further studies.

## CONCLUSION

Ongoing work is in progress, to validate how well the analysed slag compositions correspond to the measurement data from the optical emission spectrometer (OES) measurements. If the OES results agree with our results, it indicates that the OES method has the potential to provide a fast feedback on slag composition changes which could be utilised in process control.

## REFERENCES

- [1] K. Weman, Svets Handbok, 2 ed. Liber AB, 2002, ISBN 91-47-05143-4.
- [2] KTH, Institutionen för Materialvetenskap, Processmetallurgins Grunder, 2004.

## Experimental verification of different current flow scenarios in laboratory scale DC arcs

M. Aula<sup>a)</sup>, H. Pauna<sup>a)</sup>, N. Andersson<sup>b)</sup>, C. Jonsson<sup>b)</sup>, T. Fabritius<sup>a)</sup>

a) University of Oulu, Process Metallurgy Research Unit

b) KTH Royal Institute of Technology, Materials Science and Engineering  
Matti.Aula@oulu.fi

### INTRODUCTION

In electric arc furnace the electricity is transmitted from an electrode to steel bath, which conducts the current to another electrode. In AC furnace both the electrodes cyclically change from anode to cathode.

The electricity is transmitted from electrode to steel bath via slag or arc plasma. The different types of arc shapes are presented in Figure 1.

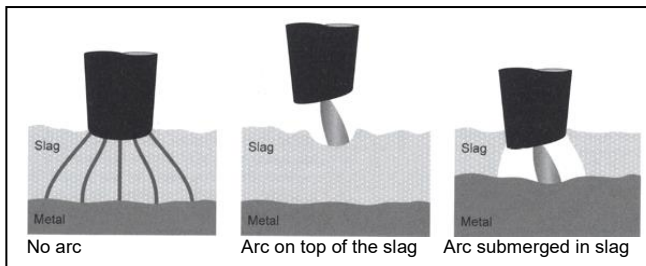


Fig. 1. Possible arrangement of current flows in EAF [1].

The main factors affecting how the current flows are the electrical conductivity of the slag, the depth of the slag and the arc voltage. With high voltage, low slag conductivity and thicker slag layer the shape in which the arc is on top of the slag becomes more probable. An example of arcs observed on top of the slag from ilmenite smelting is presented in Figure 2.

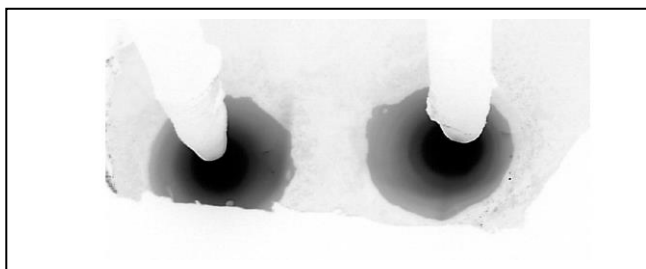


Fig. 2. An example of short, low power arcs observed during ilmenite smelting in pilot DC furnace [2].

The aim of the research was to test if these different arc shapes can be observed in laboratory furnace by manipulating the factors affecting the current flows.

### Experimental setup

The tests were conducted with an induction heating furnace situated at Royal University of Technology in Stockholm. The arc was generated on top of the slag with a system modified from a welding machine ESAB

LHH400 Universal. The behaviour of the arc was observed with two industrial grade cameras. One camera had four green glass filters and 25 ms integration time while the other had single 1050 nm filter with 0.1 ms integration time. The frames were taken with an approximate frequency of 20 Hz for the green filtered camera and 16 Hz for the 1050 nm filtered. The difference in filtering allowed measurement of different phenomena, the green filtered camera was used to observe arc shapes while the other one had better sensitivity for high temperature slag.

The differences in slag depth were created by adding more slag formers and the foaming slag conditions were generated by injecting oxygen to the furnace. The furnace and foaming tests are presented in Figure 3.

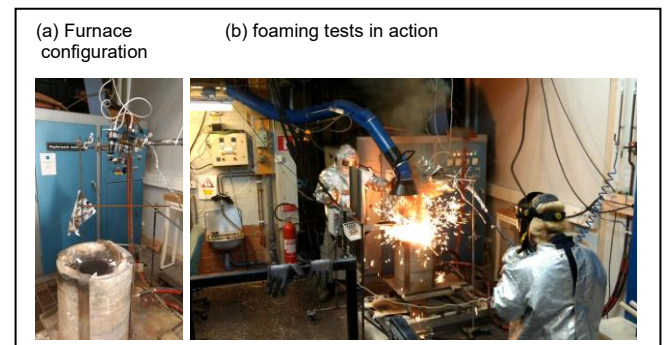


Fig. 3. Pictures from the measurement campaign.

During the heats slag formers were added in batches and the arc was generated by switching of the heating and moving the arc equipment into the furnace. During the arc tests the voltage and electrode position were varied to test their effect on the arc position.

In slag foaming tests the oxygen was injected to the furnace and the arc was generated simultaneously. The foaming also continued for some tens of seconds after the oxygen injection was turned off, thus exhibiting spontaneously foaming conditions.

### RESULTS

The experiments show that with flat bath conditions without foaming the arc is often observed on the top of the slag. This is especially common during the first additions of slag. Two bright arcs from both electrodes can be observed in Figure 4. The figure contains

processed images and colour maps, which highlight the intensity of the positions near the arc.

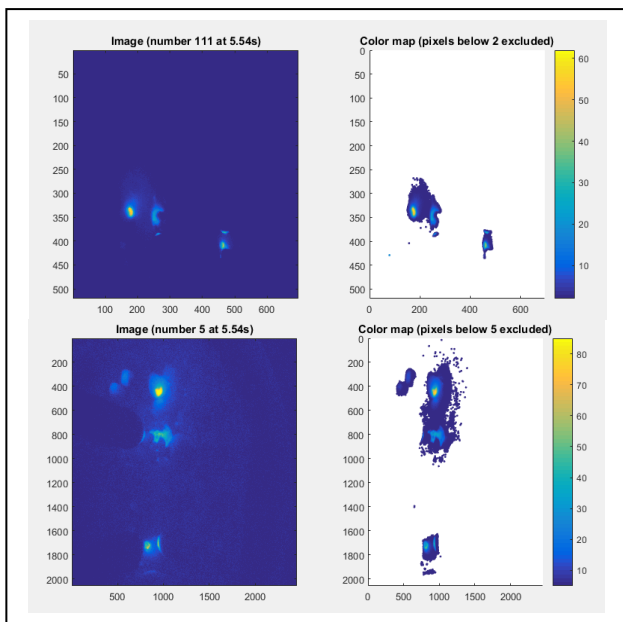


Fig. 4. Images and colour maps obtained from the two cameras (top green filtered, bottom 1050 nm filtered) during early slag additions.

In conditions with visibly low viscosity slag, it was typical to observe only a single arc despite two electrodes. The wear of the electrodes is not uniform, which causes the electrode lengths to start deviate from each other. The results is that while the other electrodes touches the slag, the other has a long arc. This type of an arc is presented in Figure 5.

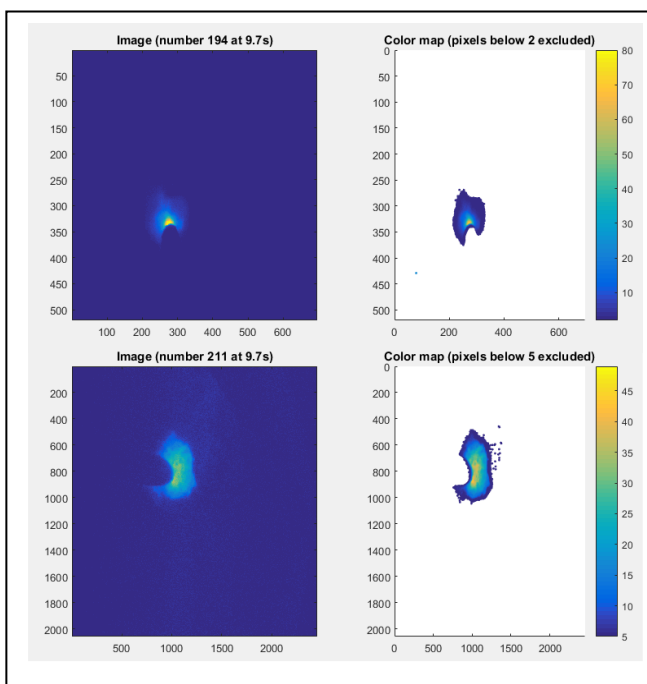


Figure 5. Images and colour maps obtained from a single arc with the two cameras (top green filtered, bottom 1050 nm filtered).

Despite constantly increasing slag amount and slag foaming, arc could be observed on top of the slag when the arc power and electrode position was varied. This can be observed from figure 6, where the shape of the oxygen lance is clearly visible. Without manipulating the electrode position the arc was submerged during the foaming.

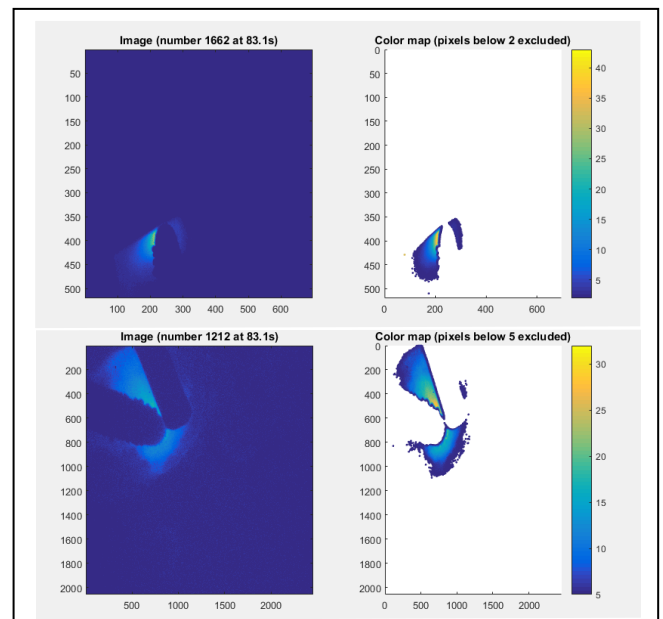


Fig. 6. Images from the two cameras and their colour map during foaming (top with green filter, bottom with 1050 nm filter).

## CONCLUSION AND OUTLOOK

The results show that despite varying slag depths and foaming conditions, the arc could be raised on top of the slag. This indicates that with the current experimental setup, the effect of the arc voltage dominates the other effects on the mode of current flow. Even with the foaming slag, a stable arc could be observed on top of the slag. With the high arc voltages, the arc can burn over the foaming slag if the foaming slag conditions are not optimal. Furthermore, this suggests that measurement techniques relying on analysis of light emitted by the arc are feasible even with foaming slag.

## REFERENCES

- [1] B. Bowman and K. Krüger: Arc Furnace Physics, Verlag Stahleisen GmbH, Düsseldorf, (2009), 247.
- [2] Q.G. Reynolds and R.T. Jones: Twin-electrode DC smelting furnaces – Theory and photographic testwork. Mintek. [White paper].

## Applications of Life Cycle Assessment for sustainable Steel Production in the Electric Arc Furnace

T. Reichel <sup>a)</sup>, M. Klein <sup>b)</sup>, M. Hauke <sup>b)</sup>, T. Echterhof <sup>a)</sup>, H. Pfeifer <sup>a)</sup>

a) RWTH Aachen University

b) ifu Hamburg GmbH  
reichel@iob.rwth-aachen.de

### INTRODUCTION

A Life Cycle Assessment (LCA) is a systematic method of analyzing and evaluating product systems, which takes into account the entire lifecycle of a product. A LCA will monitor all environmental impacts of the production, processing, use and disposal of the respective product. The results of a LCA reveal weaknesses and potentials for improvement within a product system. They also provide information on the interactions of the individual process steps, which can be used to optimize processes and increase sustainable production. During the RFCS Research project GreenEAF2 the environmental impacts of the usage of biochar during electric steelmaking in the Electric Arc Furnace (EAF) were investigated by a LCA study. [1,3]

### STRUCTURE OF AN LCA

In general, a LCA study is divided into four phases:

- goal and scope definition: defines the system, system boundary and the complexity of a study
- life cycle inventory or “life cycle Inventory phase” (LCI): a collection of process input/output data should be conducted that are contained in the defined system boundary
- life cycle impact assessment or “life cycle impact assessment” (LCIA): the collected data are transferred into environmental impacts to compare different life cycle stages with each other or compare different studies by standardization and weighting processes
- interpretation: illustrates and totalizes the results of the LCI and/or LCIA phase and refers to the defined aims from the goal and scope definition phase.

The LCA methodology is an iterative process so that all four phases have an influence on each other. [1,3]

### MODELLING

During this research project, three separate LCA models were created and evaluated. Therefore, the modelling software Umberto NXT Universal and process data by the participated steel plants were used. In a first step, all relevant input and output materials during the melting process in the EAF were considered (fig. 1). [2]

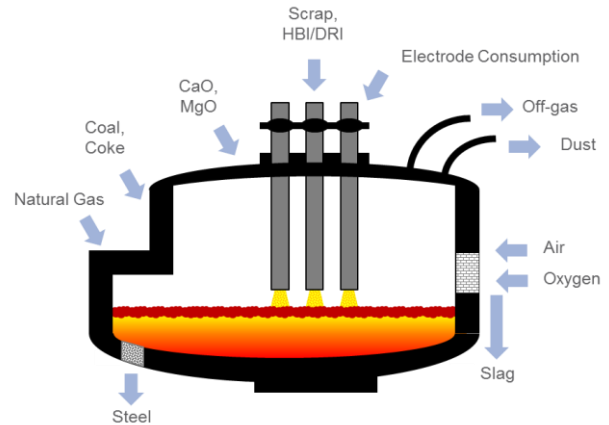


Fig. 1: General mass balance

On this basis, a general process model using the LCA software Umberto NXT Universal was created (fig. 2). The added carbon carriers were divided into biogenic and fossil additives to enable a comparison between the alternative input materials. The electric energy consumption had to be added to the model to ensure a complete calculation of the CO<sub>2</sub> intensity of the steelmaking process.

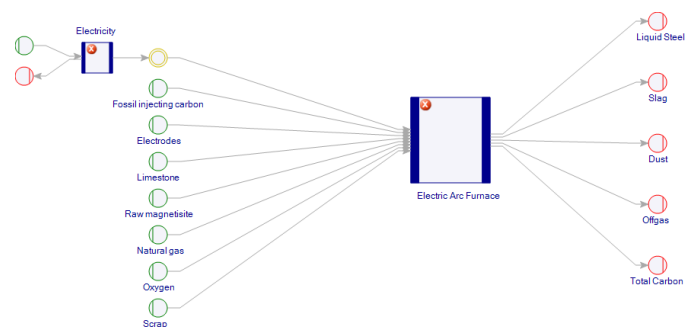


Fig. 2: Reference LCA model

The relevant process data are divided into three Groups by different scenarios concerning the kind of charged carbon:

- Sc.1: 100 % fossil carbon
- Sc.2: 50 % fossil carbon and 50 % biogenic carbon
- Sc.3: 100 % biogenic carbon

Palm kernel shells (PKS) were used as biogenic carbon carriers during the steelmaking process. With

regard to the reference process (100 % fossil carbon, scenario 1), data of 185 heats were collected and evaluated. In Case of the mixed campaign (50 % fossil carbon and 50 % biogenic carbon, scenario 2) data of 215 heats and concerning the 100% substitution trials (100 % biogenic carbon, scenario 3) data of 476 heats were collected.

**RESULTS**

During the Life cycle impact assessment aggregated CO<sub>2</sub> emission factors, off-gas composition, steel composition, slag composition and the specific electric energy consumption were analyzed.

The total CO<sub>2</sub> emissions of scenario 1 are higher in average than the corresponding value of scenario 2 and 3. The mixed campaign (50 % fossil carbon and 50 % biogenic carbon) shows the lowest CO<sub>2</sub> emissions, which means a decrease of 13.31 % in relation to scenario 1 and a decrease of 3.14 % in relation to scenario 3. Furthermore, a lower consumption of oxygen and fossil injecting carbon can be observed in scenario 2 in relation to scenario 1 and 3. If the upstream chains of oxygen were also included in this calculation, the difference in the total CO<sub>2</sub> emissions would be even higher. The biggest differences in the specific emissions are evident in the case of the electric energy consumption:

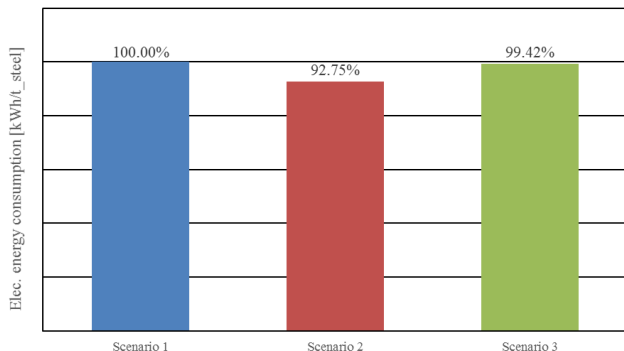


Fig. 3: Electric energy consumption

The use of PKS during the industrial tests (scenario 2 and scenario 3) has no negative consequences for the molten steel or the process control. With respect to the slag, there are also no negative influences caused by the PKS, so that the slag can continue to be used as before. During the industrial long-term trials with PKS a different reaction behavior of the biogenic carbon carriers could be observed. The biochar is characterized by a significant higher reactivity as the fossil carbon, which leads to a high average amount of CO and CO<sub>2</sub> in the off gas.

**EXTENDED MODEL**

During the Ecosteel research project an extended LCA model within all relevant upstream and downstream process of the electric steelmaking route will be developed. In collaboration with three German steel plants and the ifu Hamburg GmbH a new

modeling approach was set to build an holistic LCA study.

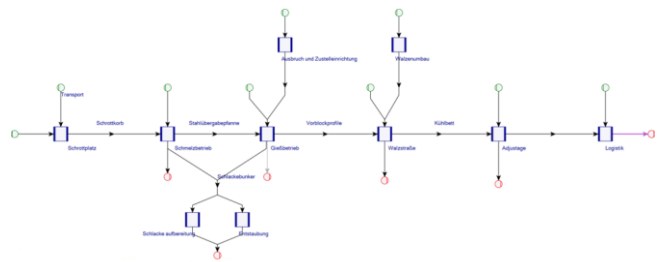


Fig. 4: Extended LCA model

The aim of the project is the development of the prototype of a software application that enables engineers in steel mills to autonomously map the steelmaking process and carry out an LCA. The process model should be able to be adapted to individual circumstances and supported by a sector-specific database.

**CONCLUSION AND OUTLOOK**

The LCA study shows the feasibility of the usage of biogenic carbon during the electric steelmaking process. The use of PKS during the industrial tests has no negative consequences for the molten steel, other output materials or the process control. The reduction concerning the specific electric energy consumption in scenario 2 shows, that the carbon footprint of the steel production in EAFs, can be reduced by substituting fossil coal with biochar. For further investigations on PKS usage in the EAF, the charging of biomass is implemented in a dynamic EAF process simulation model by Meier et al. [4]. Furthermore, an extended LCA model and a module based software prototype will be developed during the Ecosteel project.

**REFERENCES**

- [1] Klöpffer, W.; Grahl, B.: Ökobilanz (LCA)- Ein Leitfaden für Ausbildung und Beruf, WILEY- VCH Verlag, Weinheim, 2009
- [2] Pfeifer, H.; Nacke, B.; Beneke, F.: Praxis- handbuch Thermoprozesstechnik, 2. Edition, Vulkan Verlag, Essen, 2011
- [3] World Steel Association: Life cycle assessment (LCA), URL: <http://www.worldsteel.org/publications/position-papers/lca.html>, accessed on 02.02.2016
- [4] Meier, T.; Hay, T.; Echterhof, T.; Pfeifer, H.; Rekersdrees, T.; Schlinge, L.; Elsabagh, S.; Schliephake, H.: Process Modeling and Simulation of Biochar Usage in an Electric Arc Furnace as a Substitute for Fossil Coal, Steel Research int. 87 (2017) No. 9999

## **CRM EAF model development, enrichment and industrial implementations**

Jean-Christophe Pierret

CRM GROUP

Jean-Christophe.PIERRET@crmgroup.be

CRM developed a dynamic on/off-line model for the EAF process. As opposed to using statistically based calculations, the CRM model is based on a fundamental set of calculations based on thermodynamics and kinetics that takes dynamically into account furnace operating data. The purpose of the on-line application is to provide the operator with a better estimation of the melting state of the furnace and liquid steel temperatures to reduce the frequency of temperature measurements and increase the reliability of those taken. This in turn will enable lower tap temperatures and reduce energy consumption.

The model has been successfully used for off-line simulations of different furnaces and scenarios (e.g. various operating patterns). Its first on-line application was carried out at AM Esch-Belval (Luxembourg). Implementation at Dofasco plant (Canada) necessitate to enrich the model in order to allow large use of hot metal and installation at Lazaro-Cardenas plant (Mexico) required to allow 100% DRI feeding.

## Current state and ongoing development of a dynamic EAF process model

T. Hay, A. Reimann, T. Echterhof, H. Pfeifer

RWTH Aachen University, Department for Industrial Furnaces and Heat Engineering  
hay@iob.rwth-aachen.de

### INTRODUCTION

Steelmaking in the electric arc furnace (EAF) is one of the two main sources of crude steel and the main recycling route for scrap. Therefore, there is significant interest in optimization of the EAF process with regard to energy and resource efficiency, tap-to-tap time, emission control and other aspects. To gain a better understanding of the process and identify possible potential for optimization, simulation models are used.

The presented process model is based on the approach published by Logar, Dovzan and Škrjanc.[7-11] It was developed further by Meier, who implemented the electrode as a separate zone and changed the gas phase and thermal radiation models.[12] The model is analytical in nature and based on fundamental thermodynamic and physical principals. However, some empirical parameters remain necessary to describe simplified or insufficiently documented relationships. In the current implementation, the model uses data from an industrial EAF as input and for validation of the simulation results.

It is planned to attain operational data from at least two more EAF to use as model input to further validate its applicability to industrial furnace operation. Furthermore, the thermochemical calculation will be improved by including additional elements and improving the equilibrium calculation the chemical reaction rates are based on. To accelerate and ease parameterization when applying the model to different furnaces and operating conditions, an optimization algorithm is being developed and tested, that adjusts the necessary parameters.

### Thermochemical Model

In the current model the equilibrium concentrations used when calculating reaction rates are based on equilibria of different oxide species in the slag and the concentrations of metal in the melt. CaO, MgO, Al<sub>2</sub>O<sub>3</sub>, SiO<sub>2</sub>, MnO, P<sub>2</sub>O<sub>5</sub> and FeO are considered in the slag, while Si, Mn, P, C and Fe are included in the melt. The reaction rates for injected C and O<sub>2</sub> are based on the same equilibrium concentrations. The concentration and reactions of Oxygen dissolved in the melt are not considered.

In combination with the temperature, the composition of the melt is one of the main target value for the EAF process. Since the oxidation of metals releases

significant amounts of energy, the thermochemical calculation has a strong influence on both the melt's temperature and composition. To better model this aspect of the EAF process it is planned to consider Al and S in addition to the currently implemented elements and improve the calculation of the equilibrium concentrations. The oxygen concentration within the melt will be calculated. Slag and melt compositions will then be determined by the equilibrium reactions of each element with oxygen in the melt and it's oxide in the slag, with the exception of Sulphur which forms an additional anion in the slag and is treated as such.

For this purpose the regular solution model as published by Ban-Ya [1], Gaye's model [3-6] and an approach using stored equilibrium data calculated by Factsage are considered. Activities of species in the melt are calculated using the interaction parameters suggested by Sigworth and Elliot.[14]

The calculation suggested by Ban-Ya is sufficiently simplified to be executed for each step of the simulation and most of the necessary interaction parameters can be found in literature. However, the model has been criticized for being oversimplified and only accurate for narrow composition ranges.[2, 13]

While based on a similar approach of describing multi-component slags with binary interaction parameters, Gaye's model is more complex and considered to give better results.[2, 13] Depending on the execution speed for the necessary equations in Matlab it may however be too complex to be evaluated for each iteration. As with Ban-Ya's model both the necessary equations and most interaction parameters can be accessed through literature.

Both models will be implemented and compared to equilibria calculated using Factsage for the composition ranges relevant for the EAF model. Apart from accuracy, the execution speed within the model will have to be evaluated.

Another approach under consideration is storing equilibrium data for the necessary ranges of composition and temperature. This data would then be accessed from within the simulation without the need to execute the calculation for each iteration. This would allow for a more time-consuming method to be used for calculating the equilibrium conditions. To store and access the pre-calculated thermochemical data without the need for excessive storage capacity and time the

system suggested by Zietsman could potentially be applied.[15] In its current state the published system for storing and evaluating the equilibrium data through graphic representation has only been applied to ternary systems. However it is planned to further develop the method and potentially apply it to the presented EAF model.

### Parameter Optimization

The process of readjusting model parameters when applying the model to different furnaces or operating conditions, or after changes to the model have been made, can be quite time consuming and requires extensive knowledge about the model. To reduce both time and necessary knowledge, an algorithm that will automatically adjust parameters and evaluate the simulation results in comparison to plant data has been developed.

After selecting the parameters to be adjusted and the allowed range for each parameter, a combination of a genetic algorithm and local optimization is used to search for the optimal set of parameters within the given range. The quality of a solution is rated by the mean squared error between selected results calculated by the model and plant data. The genetic algorithm generates new sets of parameters in different areas of the search-space, retaining and modifying the best solutions from the previous generation, while the local optimization allows for efficient and directional searches in the vicinity of a promising solution generated by the genetic algorithm.

While the model with its non-linear behaviour and the large number of necessary parameters have proven to be too complex for global optimization, the algorithm has been useful in optimizing isolated aspects of the model and finding inconsistencies in the implementation and the use of certain parameters. Currently its use still requires significant knowledge of both the model and the algorithm. Therefore, further development is necessary, but there may be potential to accelerate the process of parameterization.

### REFERENCES

- [1] **Ban-Ya, S.:** Mathematical Expression of Slag-Metal Reactions in Steelmaking Process by Quadratic Formalism Based on the Regular Solution Model, *ISIJ International* Vol. 33 (1993) No. 1, pp. 2-11
- [2] **Costa e Silva, A.:** An Overview of the Use of Calphad Methods in Steelmaking, *Journal of Mining and Metallurgy* Vol. 35 (1999) No. 1B, pp. 85-111
- [3] **Gaye, H.; Faral, H.:** Metal Slag Equilibria, *Proceedings of Second International Symposium in Metallurgical Slags and Fluxes, Lake Tahoe, USA, p. 159-179*
- [4] **Gaye, H.; Lehmann, J.; Matsumiya, T.; Yamada, W.:** A Statistical Thermodynamics Model of Slags: Applications to Systems Containing S, F, P<sub>2</sub>O<sub>5</sub> and Cr Oxides, *Proceedings of 4th International Conference on Molten Slags and Fluxes, Sendai, Japan, 1992, p. 103-108*
- [5] **Gaye, H.; Welfringer, J.:** Modelling of the Thermodynamic Properties of Complex Metallurgical Slags, *Proceedings of Second International Symposium in Metallurgical Slags and Fluxes, Lake Tahoe, USA, p. 357-375*
- [6] **Lehmann, J.; Gaye, H.; Rocabois, P.:** The IRSID Slag Model for Steelmaking Process Control, *Proceedings of 2nd International Conference on Mathematical Modeling and Computer Simulation of Metal Technologies, MMT2000, Ariel, Israel, 2000, p. 89-96*
- [7] **Logar, V.; Dovžan, D.; Škrjanc, I.:** Mathematical modeling and experimental validation of an electric arc furnace, *ISIJ International* Vol. 51 (2011) No. 3, pp. 382-391
- [8] **Logar, V.; Dovžan, D.; Škrjanc, I.:** Modeling and Validation of an Electric Arc Furnace Part 1, Heat and Mass Transfer, *ISIJ International* Vol. 52 (2011) No. 3, pp. 402-412
- [9] **Logar, V.; Dovžan, D.; Škrjanc, I.:** Modeling and Validation of an Electric Arc Furnace Part 2, Thermo-chemistry, *ISIJ International* Vol. 52 (2012) No. 3, pp. 413-423
- [10] **Logar, V.; Škrjanc, I.:** Development of an Electric Arc Furnace Simulator Considering Thermal, Chemical and Electrical Aspects, *ISIJ International* Vol. 52 (2012) No. 10, pp. 1924-1924
- [11] **Logar, V.; Škrjanc, I.:** Modeling and Validation of the Radiative Heat Transfer in an Electric Arc Furnace, *ISIJ International* Vol. 52 (2012) No. 7, pp. 1225-1232
- [12] **Meier, T.:** Modellierung und Simulation des Elektrolichtbogenofens, *Fakultät für Georessourcen und Materialtechnik der Rheinisch-Westfälischen Technischen Hochschule Aachen, Mainz, 2016*
- [13] **Ortel, L. C.; Costa e Silva, A.:** Application of Thermodynamic Modeling to Slag-Metal Equilibria in Steel Making, *Calphad* Vol. 23 (1999) No. 3, pp. 379-391
- [14] **Sigworth, G. K.; Elliot, J. F.:** The Thermodynamics of Liquid Dilute Iron Alloys, *Metal Science* Vol. 8 (1974), pp. 298-310
- [15] **Zietsman, J. H.:** Efficient Storage and Recall of Slag Thermochemical Properties for Use in Multiphysics Models, *Proceedings of Conference on Molten Slags, Fluxes, and Salts (MOLTEN16), p. 635-644*

## Determining the critical modelling parameters in a simplified EAF arc-heat distribution model

Suzanne Roberts, Thomas Echterhof, Herbert Pfeifer

Department of Industrial Furnaces and Heat Engineering, RWTH Aachen University  
 roberts@iob.rwth-aachen.de

### INTRODUCTION

The melting and refining of scrap and iron containing metal in electric arc furnaces (EAFs) is currently the second largest steel production process globally, and approximately 29% of the steel produced in the world is being produced in EAFs<sup>[1]</sup>. With world crude steel production increasing by 5.3% from 2016 to 2017<sup>[2]</sup>, it is becoming increasingly desirable to design and operate EAFs as efficiently, economically and environmentally friendly as possible. A step towards this goal is minimizing heat losses to the off-gas and the environment, and in order to achieve this, the heat transfer processes inside an EAF should be well-understood. An improved understanding of the heat transfer processes inside EAFs could additionally aid planning for maintenance work and could lead to furnace design and operation practices that would increase the lifetime of furnace components.

Mathematical modelling is well-suited to the investigation of the heat transfer processes taking place inside EAFs, since the aggressive, high-temperature environment inside arc furnaces limits experimental measurement opportunities. In this work a low computational-complexity EAF arc-heat distribution model is implemented and used to study the sensitivity of the modelled heat distribution to changes in model parameters.

### MODEL PARAMETER SENSITIVITY STUDY

The low computational-complexity EAF arc-heat distribution model of Fathi et al. as described in [3] is implemented and arc-heat distribution predictions from the model implementation are successfully verified against the model results reported by Fathi et al.<sup>[3]</sup> The implemented model predictions agree to within a tenth of a percent to the published results. For the purposes of the sensitivity study, the model parameters are varied and the effect on the arc-heat distribution is investigated over an arc current range of 1 – 90 kA and an arc length range of 5 – 100 cm.

In Figure 1 the percentage of the heat transferred from the arc in the form of arc electron flow (green), convective power (blue) and radiative power (yellow) is plotted against arc length. The varied parameter in Figure 1 is the current density at the cathode spot. Different parameter values are indicated by the different line styles. In Figure 2 the anode work function is the parameter that is varied. It can be seen from comparing Figures 1 and 2, that a change in the

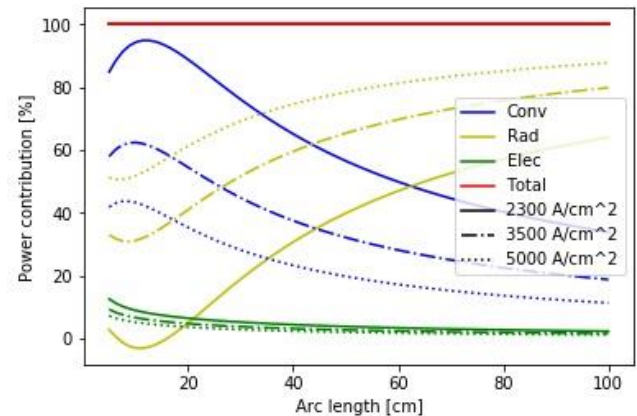


Fig. 1 Sensitivity of the arc power distribution w.r.t. the current density at the cathode spot.

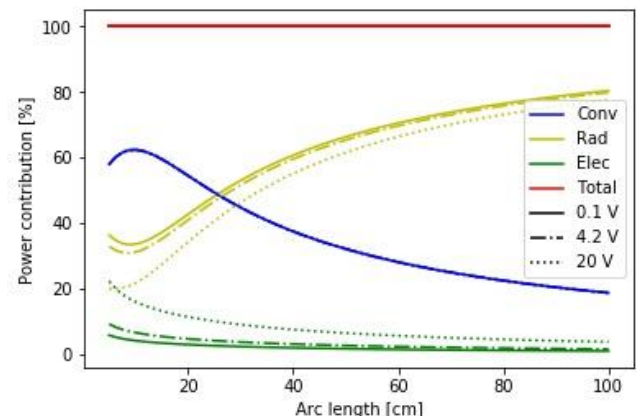


Fig. 2 Sensitivity of the arc power distribution w.r.t. the anode work function.

value of the current density at the cathode spot has a considerable influence on the arc-heat distribution, while variations in the anode work function only result in changes of 10% or less for each form of power dissipation over the investigated range of arc lengths. The same parametric study is conducted for various parameters (listed as independent variables in Figure 3), resulting in plots similar to Figures 1 and 2. Apart from this sensitivity study conducted over a range of arc lengths, a similar sensitivity study is also conducted over a range of arc currents.

### RESULTS

Figure 3 summarizes the results of the parametric study on both a range of feasible currents and a range of feasible arc lengths. The maximum difference

between the percentage power radiated from the arc in the base case, and the percentage power radiated when a parameter value is varied, is plotted. Only the parameter sensitivity to radiation heat transfer is plotted, since the variation in heat transfer through arc electron flow is generally around ten percent or less (see e.g. the green plots in Figures 1 to 2), and the sum of the electron flow, convection and radiation heat transfer must always be 100%. Therefore, the convection heat transfer variation only differs with ten percent or less from the radiation heat transfer variation and consequently the effect of a parameter change on only one of these two heat transfer modes is considered to be representative of its effect of both.

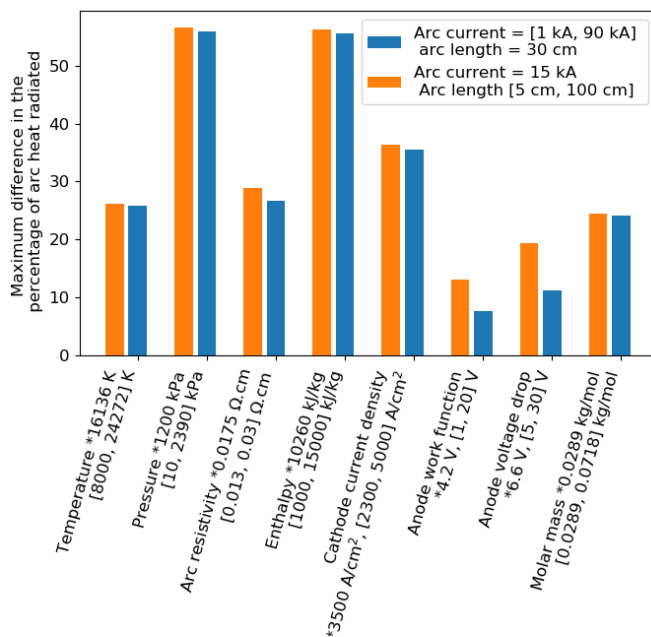


Fig. 3 Parameter sensitivity across an arc current range of 0 – 90 kA. Investigated parameter ranges are indicated in square brackets and base case values with a \*.

It can be seen in Figure 3 that changes in the parameters describing the arc pressure, and the enthalpy change between the arc and the freeboard gas, result in the biggest variations of about 55% in the predicted arc-heat distribution. The values of the anode work function and the anode voltage drop has a minimal influence on the arc-heat distribution – 20% or less over the arc length range and 12% or less when the range of arc currents is considered. Considering the stochastic nature of the arc and the large amount of variation and uncertainty this introduces to most of the parameters used in an arc model, it is concluded that it is not initially necessary to model these phenomena in more detail.

Furthermore, Figures 1 and 2 are representative of the majority of plots of power contribution versus arc current or arc length obtained in the sensitivity study. It is generally notable that the percentage power contributed by electron flow is largely unaffected by

changes in parameter values. The largest changes in electron flow heat transfer are observed for the anode voltage drop and anode work function (Fig. 2) parameters, with a variation of about 15% at very short arc lengths.

It is further interesting to note that generally, and as is also the case in Figures 1 and 2, radiation is the dominant heat transfer mode at low currents and long arc lengths, but convection is dominant at large currents and short arc lengths. The fact that convection can be a dominant heat transfer mode for the high temperature process rather than radiation, despite it being a fourth power function of temperature, can possibly be attributed to the high velocities in the arc.

## CONCLUSION AND OUTLOOK

A simplified EAF arc-heat distribution model is implemented and used to investigate the arc-heat distribution's sensitivity to the various model parameters. The advantages of a simplified model is that it provides quick approximations and is useful for investigating the large number of scenarios required for a sensitivity study.

Both convection (at large currents and short arc lengths) and radiation (at low currents and long arc lengths) heat transfer are found to be dominant modes of heat transfer from the arc. The arc-heat distribution is found to be especially sensitive to the model parameters describing the arc pressure and enthalpy change between the arc and the freeboard gas. On the other hand, it is minimally sensitive to the model parameters describing the voltage drop and work function at the anode.

These results will be used to inform model decisions in planned subsequent more detailed models. The availability of both simpler, computationally cheap models and higher fidelity, computationally expensive models will then allow for multi-fidelity modelling investigations.

## REFERENCES

- [1] World Steel Association (worldsteel), About Steel, retrieved on 30 January 2018 from <https://www.worldsteel.org/media-centre/about-steel.html>
- [2] World Steel Association (worldsteel), Media center, Press releases, World crude steel output increases by 5.3% in 2017, 24 January 2018, Brussels, Belgium, retrieved on 30 January 2018 from <https://www.worldsteel.org/media-centre/press-releases/2018/World-crude-steel-output-increases-by-5.3--in-2017.html>
- [3] Fathi A, Saboohi Y, Škrjanc I, and Logar V., 2015, Low Computational-complexity Model of EAF Arc-heat Distribution, ISIJ International, Vol. 55, No. 7, pp 1353-1360.

REVIEW ON STATISTICAL ENERGY DEMAND MODELS FOR THE EAF AS PROCESS EVALUATION TOOLS

T. Echterhof

RWTH Aachen University, Department for Industrial Furnaces and Heat Engineering  
 echterhof@iob.rwth-aachen.de

INTRODUCTION

Efforts to optimize the steelmaking process in the EAF are difficult to evaluate because of the overall variability of the EAF steelmaking process. In addition, some varying boundary conditions of the process are still difficult to determine like scrap quality, water content of the scrap, slag foaming, hot heel.

Hence and since the available analytical models are still limited, for practical use a number of statistical or empirical models were developed and will be presented and discussed in the presentation.

ENERGY DEMAND MODELS

A number of empirical models for the prediction of the energy demand of EAFs in the steel industry were developed in the recent decades. Some predict the overall energy demand, most predict the specific electrical energy demand.

Köhle<sup>[1]</sup> was the first to publish in 1992 an empirical model for the electrical energy demand of electric arc furnaces. The model can be used to determine the specific electrical energy demand of an EAF process  $W_R$  in kWh/t from typical operational data of the heat:

$$W_R = 300 \frac{kWh}{t} + 900 \frac{kWh}{t} \left[ \frac{G_E}{G_A} - 1 \right] + 1600 \frac{kWh}{t} \frac{G_Z}{G_A} + 0.7 \frac{kWh}{t \cdot K} [T_A - 1600^\circ C] + 0.85 \frac{kWh}{t \cdot min} t_C - 8 \frac{kWh}{m^3} M_G - 4.3 \frac{kWh}{m^3} M_L \quad (1)$$

with

$W_R$	Specific electrical energy demand, calculated with the model [kWh/t]	$t_C$	Heat duration from power-on to begin of tapping [min]
$G_A$	Furnace tap weight [t]	$T_A$	Tapping temperature [°C]
$G_E$	Weight of all ferrous materials [t]	$M_G$	Specific burner gas [m <sup>3</sup> /t]
$G_Z$	Weight of slag formers [t]	$M_L$	Specific lance oxygen [m <sup>3</sup> /t]

The model assumes a linear dependency of the specific electrical energy demand from process parameters and input materials. The coefficients of equation (1) were determined by linear regression to process data of 14 different EAFs with tapping weights between 64 t and 147 t. The process data used for the statistical analysis were average data gathered between end 1990 and beginning of 1991 of all 14

furnaces as well as data from numerous heats of two of the 14 EAFs. All of the furnaces investigated operate on 100% scrap and are not using any form of scrap preheating.

After subsequent steps of development, Köhle<sup>[2]</sup> presented in 2002 the up to now final revision of the electrical energy demand model. The changes in comparison to the first model published in 2000 is the addition of coefficients taking the amount of charged DRI, HBI, hot metal and shredded scrap into account. In addition, coefficients related to the specific consumption of oxygen for post-combustion and related to energy losses were added in equation (2).

$$\frac{W_R}{kWh/t} = 375 + 400 \left[ \frac{G_E}{G_A} - 1 \right] + 80 \frac{G_{DRI/HBI}}{G_A} - 50 \frac{G_{Shr}}{G_A} - 350 \frac{G_{HM}}{G_A} + 1000 \frac{G_Z}{G_A} + 0.3 \left[ \frac{T_A}{^\circ C} - 1600 \right] + 1.0 \frac{t_S + t_N}{min} - 8.0 \frac{M_G}{m^3/t} - 4.3 \frac{M_L}{m^3/t} - 2.8 \frac{M_N}{m^3} + NV \frac{W_V - W_{Vm}}{kWh/t} \quad (2)$$

with the additional values

$G_{DRI}$	Weight of DRI [t]	$t_N$	Power-off time [min]
$G_{HBI}$	Weight of HBI [t]	$M_N$	Specific oxygen for post-combustion [m <sup>3</sup> /t]
$G_{Shr}$	Weight of shredder [t]	$W_V$	energy losses (if measured)
$G_{HM}$	Weight of hot metal [t]	$W_{Vm}$	mean value of $W_V$
$t_S$	Power-on time [min]	$NV$	furnace specific factor (0.2 ... 0.4)

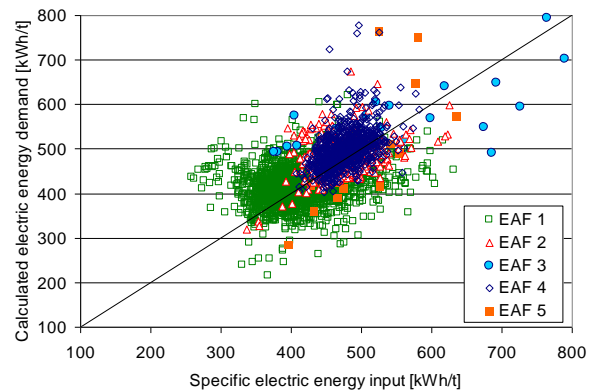


Fig. 1 Comparison of calculated electrical energy demand with real data from five EAFs in Europe, all charged with 100% steel scrap and alloys, partly high alloyed<sup>[3]</sup>

The application of the model by Kirschen et al.<sup>[3]</sup> to five European EAFs showed very good predictive capabilities of the model with regard to average values. For the prediction of the electrical energy demand of single heats on the other hand, the model is less suitable due to the high scatter visible in Fig. 1.

### EAF SPECIFIC ENERGY DEMAND MODELS

Kirschen et al.<sup>[4]</sup> discuss the adaption of the Köhle model to specific furnaces as well as an entirely new furnace specific regression model in comparison to the Köhle model. They show results for an EAF charged with scrap, cold and hot DRI. Since the use of hot DRI is not included in the Köhle model, a completely new furnace specific model is created by a stepwise multiple linear regression. The model is based on available operational data. Therefore additional data not present in the Köhle model (e.g. metal yield, charged carbon, etc.) is used on the one hand side, while other data is not used because of missing relevance for the process (e.g. hot metal, shredder, etc.) or because of statistical insignificance for the model (e.g. tapping temperature). The model resulting from the stepwise multiple linear regression is given in equation (3).

$$\begin{aligned} \frac{W_R}{kWh/t} = & -152.56 + 4.2146 \frac{G_E}{t} - 5.0795 \frac{G_A}{t} - \\ & 1.447 \frac{G_{HDRI}}{t} - 1.3039 \frac{G_{CDRI}}{t} - 1.9784 \frac{G_{Scrap}}{t} + \\ & 3.0905 \frac{G_A}{G_E} + 0.48352 \frac{t_{ttt}}{min} + 4.8648 \frac{t_S}{min} - \\ & 0.46807 \frac{t_N}{min} - 0.31964 \frac{t_{prep}}{min} - 0.0040591 \frac{M_{O2}}{m^3} + \\ & 6.8737 \frac{G_{chC}}{t} + 4.7919 \frac{G_{injC}}{t} + 3.9598 \frac{G_{Lime}}{t} + \\ & 1.3675 \frac{G_{Dolo}}{t} + 3.8739 \frac{P_{AVG}}{MW} \end{aligned} \quad (3)$$

where  $W_R$ ,  $G_E$ ,  $G_A$ ,  $t_S$ ,  $t_N$  are the same process parameters as in equation (2), and:

$G_{Scrap}$	Weight of Scrap [t]	$t_{ttt}$	Tap-to-tap time [min]
$G_{HDRI}$	Weight of hot charged DRI [t]	$t_{prep}$	Preparation time [min]
$G_{CDRI}$	Weight of cold charged DRI [t]	$M_{O2}$	Total oxygen [m <sup>3</sup> ]
$G_{chC}$	Weight of charge carbon [kg]	$G_{Dolo}$	Weight of dolomite [kg]
$G_{injC}$	Weight of injected carbon fines [kg]	$P_{AVG}$	Average power [MW]
$G_{injC}$	Weight of injected carbon fines [kg]		

Fig. 2 shows results for the EAF calculated with the Köhle model and with the new regression model. While the  $R^2$  value and the root mean squared error (RMSE) of the Köhle model is 0.31 and 74.4, respectively, the new regression model has  $R^2$  and RMSE values of 0.96 and 10.7. Apart from the high accuracy also for single heats for this specific furnace, the stepwise multiple linear regression delivered additional information with regard to the statistical relevance of various process parameters to the electrical energy demand of the EAF.

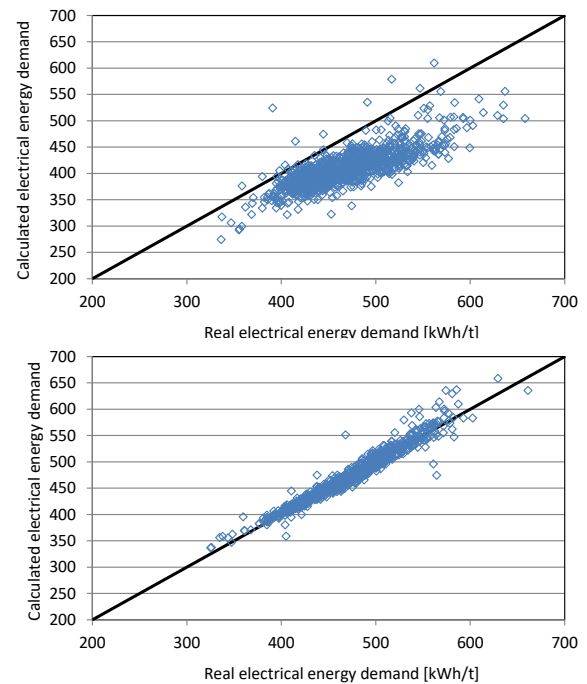


Fig. 2 Real specific electrical energy demand compared to the calculated values calculated with the Köhle model (top) and the new regression model (bottom) <sup>[4]</sup>

### CONCLUSION AND OUTLOOK

An interesting application of the energy demand models, independent of their accuracy regarding single heats, is the comparison of production and/or trial campaigns at a furnace. Given that most of the influencing factors are unchanged or fluctuating in the usual range, differences in the electrical energy demand can become visible.

When an EAF specific energy demand model is created by statistical regression, it can also give interesting insights and starting points for further discussions and investigations just by looking at what process parameters have a statistically significant or insignificant influence on the electrical energy demand of the steelmaking process in the EAF.

### REFERENCES

- [1] S. Köhle, *stahl und eisen* **1992**, 112, 59–67.
- [2] S. Köhle, in *7th European electric steelmaking conference* (Ed: Associazione Italiana di Metallurgia), AIM, Milano **2002**, pp. 1305–1314.
- [3] M. Kirschen, J.-P. Simoes, H. Pfeifer, *elektrowärme international* **2005**, 63, 89–96.
- [4] M. Kirschen, K.-M. Zettl, T. Echterhof, H. Pfeifer, in *11th European Electric Steelmaking Conference & Expo* **2016**, pp. 1–10.